RESEARCH ON AGRICULTURAL VEHICLE SAFETY WARNING SYSTEM BASED ON LIDAR

/

基于激光雷达的农业车辆安全预警系统研究

Weiyu KONG [1),2)], Guangrui HU [1)], Shuo ZHANG [1)], Jianguo ZHOU [1)], Zening GAO [1)], Jun CHEN *[1)]

[1)] College of Mechanical and Electronic Engineering, Northwest A&F University, Yangling 712100, China;

[2)] AVIC Zhonghang Electronic Measuring Instruments Co.,ltd., Xi 'an 710119，China

Tel: +86 13572191773; E-mail: chenjun_jdxy@nwsuaf.edu.cn

DOI: https://doi.org/10.35633/inmateh-68-23

Keywords: *Agricultural vehicle, Lidar, Safe distance, Pre-warning*

ABSTRACT

Intelligent agricultural vehicles have been widely used in the process of farming and harvesting in the field, which has brought great convenience to agricultural production. However, there are also safety issues such as accidental collision of agricultural vehicles or other agricultural machinery during operation. The use of sensing technology for the timely and accurate detection and pre-warning of obstacles during the operation of agricultural machinery is critically important for ensuring safety. In this paper, a two-dimensional Lidar is used to detect obstacles in front of tractors with the Density-Based Spatial Clustering of Applications with Noise (DBSCAN) algorithm and the Minimum Cost Maximum Flow algorithm (MCMF). A method to judge whether the obstacle is static or dynamic and a classification model of different security warning levels for obstacles in different states is proposed. Actual vehicle tests were conducted, with static obstacles tested repeatedly, and dynamic obstacles tested at different directions and speeds. The results showed that the overall average warning accuracy rate is 90.5%. Prediction results were robust for obstacles in different states, indicating that this system is able to ensure the safety of agricultural vehicles during their operation and promoted the development of agricultural mechanization.

摘要

智能化农业车辆在田间耕作和收获过程中已广泛使用，给农业生产带来了极大地便利。然而，还存在着在作业过程中农业车辆误撞人或其他农业机械等安全问题。利用传感技术，及时、准确地对作业农业车辆周围的障碍物进行检测和预警就有着重要的作用和意义。本文利用二维激光雷达，结合 DBSCAN 点云聚类算法和最小费用最大流算法对障碍物进行检测和追踪，提出了判断障碍物状态的方法并对不同状态的障碍物提出对应的安全预警级别划分模型。最后进行了实车试验，对静态障碍物进行了多次重复试验，对动态障碍物进行了不同方向不同速度的多次重复试验，整体的预警准确率均值为 90.5%。试验结果表明对不同状态的障碍物均取得了良好的预警效果,推动了农业机械化事业的发展。

INTRODUCTION

With the continuous development of electronic control technology and sensing technology, the degree of automation and intelligence of agricultural machinery and equipment has been continuously improved rapidly. Drones equipped with sensors can estimate crop yields (*García-Martínez et al., 2020*) and electric vehicles work together to harvest (*Loukatos et al., 2021*). They all have brought a lot of convenience to agricultural production. However, accidents frequently occur during the operation of agricultural vehicles. For example, accidents in which tractors collide with obstacles, people, or animals during their operation in the field can be fatal, damage agricultural vehicles, and lead to significant economic losses. The safety production of agricultural vehicles is thus critically important.

Several studies have examined the anti-collision safety pre-warning system in the automotive field. *Jeong et al.* proposed a safety warning information system that can provide warning messages about impending dangers by using a networked vehicle environment, thereby increasing the driver's attention (*Jeong et al., 2015*). Liu et al. proposed a pre-warning algorithm for the vehicle collision avoidance time based on vehicle speed. The algorithm sets different safe collision avoidance times according to different vehicle speeds. Furthermore, it judges whether warnings are needed by comparing the safe collision avoidance time with the time required for the vehicle to collide (*Liu et al., 2017*).

Tak et al. studied a new type of collision warning system that describes the vehicle movement handled by the roadside unit. The proposed collision warning system based on segment information overcomes the limitations of existing collision warning systems (*Tak et al., 2020*). The above research environment is the urban road traffic environment. They all need to install sensors on the vehicle and the vehicle being detected to obtain its information and make an early warning. In the farmland environment, the types of obstacles that appear are random, and may be people or livestock, not necessarily other agricultural vehicles, so they are not suitable for farmland environments.

Few studies have examined anti-collision and safety pre-warning systems in the context of agricultural production and agricultural vehicles. Zhao studied the BDS-based cross-border system for agricultural vehicles involved in soil preparation operations. Guo et al. designed a hierarchical cross-border early warning system with cross-border prediction function. Zhu et al. studied the rollover warning of heavy vehicles (*Zhao, 2019; Guo et al., 2019; Zhu et al., 2011*). Kubota Corporation of Japan developed a classification for the dangerous warning areas for its smart tractors, but the relationship between moving objects and the tractor has not been considered, which has likely caused some unnecessary alarms. Kapilan's research involves automatic accident alerts in the event of a vehicle accident. Once a specific vehicle has an accident, the proposed system will detect it and immediately send an alert containing the required information to a certain registered number (*Kapilan et al., 2020*). It can be seen that the research on the safety early warning of agricultural vehicles is still lacking.

In addition, environmental information perception is an indispensable and important link in the safety early warning system. Perceiving the surrounding environment not only requires detecting obstacles but also tracking and predicting the trajectory of dynamic obstacles. MCMF algorithm has also been widely used in wireless network control load, large-scale resource scheduling, and multi-target tracking (*Sun et al., 2014; Chen et al., 2017; Liang et al., 2019*). It achieved good results, solved the problem of finding the optimal path in the network structure, and can be used to track objects in the point cloud of the Lidar. Cao et al. improved DBSCAN to improve the accuracy of multi-radar perception of the environment of autonomous vehicles (*Cao, Wang, 2016*), However, multiple radars are used and the cost is high.

Asvadi et al. used only a three-dimensional radar and positioning and navigation equipment to detect common static and dynamic obstacles in the urban road environment, and the test results verified the feasibility of this method (*Asvadi et al., 2016*). However, the large amount of 3D Lidar data requires high performance of the processor, which results in high costs and does not meet the requirements of agricultural production. Campos et al. used the machine vision system on the tractor driving in the corn field to detect unexpected obstacles or elements in the video sequence, but this method requires higher ambient light (*Campos Y. et al., 2016*). Corno proposed an adaptive positioning system based on ultrasonic car sensors for the autonomous navigation of agricultural tractors in vineyards, but the accuracy of ultrasonics will change under the influence of temperature (*Corno et al., 2021*). Therefore, two-dimensional Lidar is used to detect obstacles in the farmland environment.

Therefore, in view of the characteristics of the field environment where agricultural vehicles are operating, this paper proposes a two-dimensional Lidar-based classification algorithm for agricultural vehicle safety warning levels. It takes into account the randomness of obstacles movement in the farmland environment. A system is then designed and tested to verify its warning accuracy and assess its applicability. The aim of this system is to reduce the occurrence of accidents during the operation of agricultural vehicles to ensure the safety of production personnel and production equipment as well as promote the development of agricultural mechanization.

MATERIALS AND METHODS

Research platform

The research platform uses the Oubao 4040 tractor. The front wheels of the tractor are turned to the rear wheels to drive. The agricultural vehicle safety pre-warning system is divided into three parts: perception, decision-making, and execution. The sensing part is the UST-20LX two-dimensional Lidar (detection range: 270°; scanning frequency: 0.25 s; angular resolution: 0.25°; HOKUYO Co., Japan) and Xingwang Yuda XW-GI5610 Beidou navigation equipment (sampling frequency: 10 Hz; manufactured by StarNeto Co., Ltd., China). The controller of the decision-making part is personal computer (PC). It is a host computer that is responsible for receiving sensor data, processing data, and making decisions. As the lower computer, Arduino Uno is responsible for receiving the signal from the upper computer to control the actuator.

The executive part is an LED alarm with red, yellow, and green lights and a buzzer. The buzzer can be combined with any colour of light to generate an alarm signal.

The LIDAR sensor is connected to the PC network port through a network cable for network port communication. BDS and PC, upper computer and lower computer are all serial communication devices. The GPIO port of Arduino is connected to the relay to control the on and off of the sound and light alarm. The sensor layout of the system is shown in Figure 1.

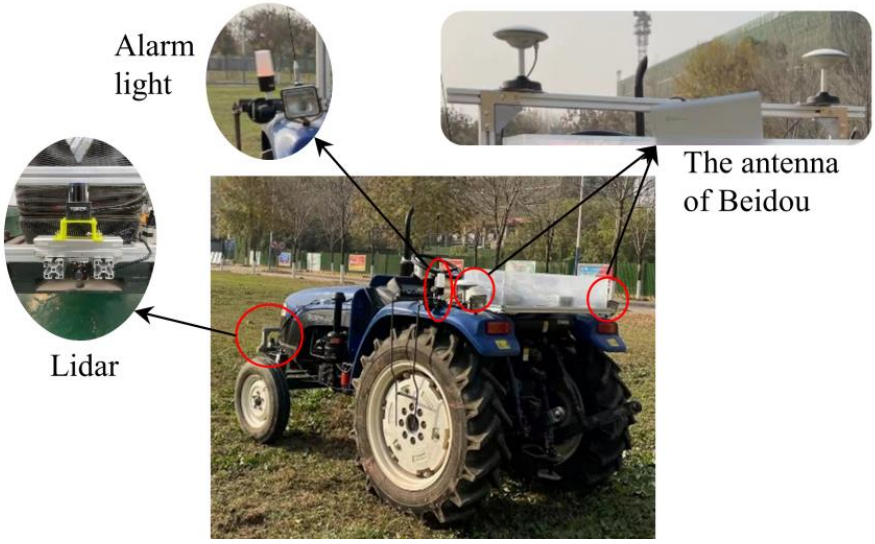

Fig. 1 - Schematic diagram of the overall structure of the system

Coordinate System

The coordinate system shown in Figure 2 is set, namely the tractor coordinate system $X_TY_TZ_T$, the laser coordinate system $X_LY_LZ_L$ and the map coordinate system XYZ.

In the laser coordinate system $X_LY_LZ_L$, the origin O_L of the laser coordinate system is the centre of the laser line emitted by the laser radar, the Y_L axis is pointing to the front of the laser radar along the 135° direction of the laser beam, and the X_L axis is along the 45° direction of the laser beam. Pointing to the right side of the Lidar, the Z_L axis is perpendicular to the plane formed by the X_L axis and the Y_L axis.

The tractor coordinate system $X_TY_TZ_T$ is the mobile station coordinate system of BDS. The position of the coordinate system changes with the movement of the tractor. The origin O_T is the installation position of the mobile station, the X_T axis points to the right along the line connecting the installation positions of the two antennas, the Z_T axis is perpendicular to the ground and upwards, and the Y_T axis is perpendicular to the plane formed by the X_T axis and the Z_T axis.

In the absolute coordinate system XYZ, the starting point of the tractor is taken as the origin O, X, Y, Z axes point to true north, true east, and vertical ground upwards, respectively. First, obtain the coordinates of the tractor in the absolute coordinate system by analysing the BDS data, and then obtain the relationship between the laser coordinate system and the tractor coordinate system from the relative position of the laser radar and the BDS installation.

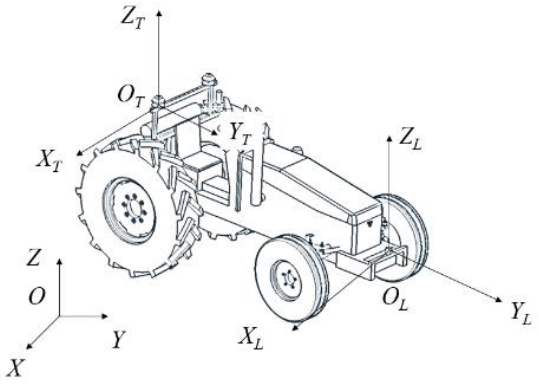

Fig. 2 - Coordinate system

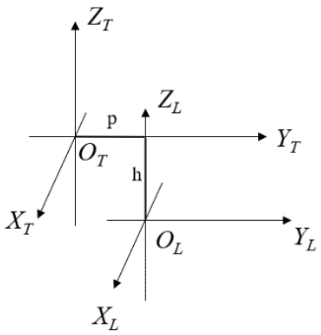

Fig. 3 - The geometric relationship between the laser coordinate system and the tractor coordinate system

As shown in Figure 3, p is the difference between O_T and O_L along the Yaxis; h is the difference between O_T and O_L along the Z axis. Therefore, the conversion relationship between the coordinates (x_L,y_L,z_L) in the laser coordinate system and the coordinates of the tractor body coordinate system (x_T, y_T, z_T) can be obtained as

$$\begin{bmatrix} x_T \\ y_T \\ z_T \end{bmatrix} = \begin{bmatrix} x_L \\ y_L \\ z_L \end{bmatrix} + \begin{bmatrix} 0 \\ p \\ -h \end{bmatrix} \quad (1)$$

$$x_L = \rho \cos\theta \quad (2)$$

$$y_L = \rho \sin\theta \quad (3)$$

The polar coordinates of the Lidar point cloud are converted to coordinates in the plane rectangular coordinate system through formulas (2) and (3). Among them, ρ is the distance between the object detected by the Lidar and the Lidar, and θ is the angle between the laser beam and the 0° line. In addition, the CGCS2000coordinates provided by BDS are converted to Gaussian plane coordinates by Gaussian orthographic projection (*Liu, 2018*).

Lidar point cloud clustering based on DBSCAN

DBSCAN is a density-based clustering algorithm. A clustering category is obtained by classifying closely connected samples into one category (*Yan W Y, et al., 2016*). All of the closely connected samples are divided into different categories, and the final results of all cluster categories are obtained. Therefore, for high-density data such as Lidar point clouds, DBSCAN clustering is used. In addition, compared with other clustering algorithms, DBSCAN has the advantages of not requiring inputs such as the number of clusters and the shape of clusters (*Zhang Y.H., et al., 2017*).

The system uses the point cloud library (PCL) to process point cloud data. First, clusters are searched by checking the Eps neighborhood of each point in the Lidar data. If the Eps neighborhood of point p contains more points than MinPts, then a cluster with p is created as the core object, and objects that are directly accessible from these core objects are iteratively gathered. This process sometimes involves the merging of clusters with reachable density. When no new points are added to any clusters, the process ends. Different colors are then added to the point cloud clusters of different objects. After visualization in Rviz, the approximate shapes and positions of different objects in the point cloud can be intuitively observed (Fig. 4).

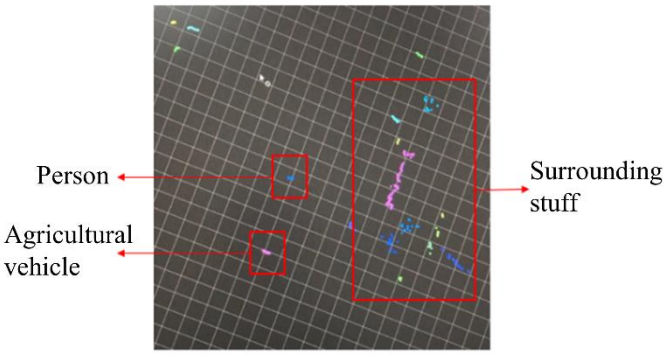

Fig. 4 - Point cloud clustering renderings

Obstacle tracking

To ensure that safety warnings for both static and dynamic obstacles are accurate, the dynamic obstacles need to be tracked to obtain various types of information, such as their movement status. The idea in this research is based on the DeepSort tracking algorithm. It uses Euclidean distance as the position metric (*Buczkowska et al., 2019*) and the MCMF to perform data association and applies them to the laser point cloud to track the objects detected by the laser to prepare for safety pre-warning.

In the position measurement, Euclidean distance is used to evaluate the degree of matching between the state predicted by the Kalman filter and the actual state.

$$\rho=\sqrt{(x_2-x_1)^2+(y_2-y_1)^2} \tag{4}$$

(x_1, y_1) and (x_2, y_2) represents the coordinates of two points, and ρ represents the Euclidean distance between these two points.

The DeepSort algorithm is applied to the image and uses the position of the detection frame for calculation (*Wojke et al., 2017*). For the point cloud data of Lidar, the position of the detection frame is replaced with the coordinates of the point cloud clustering center for calculation. The Kalman filter is used for target motion state estimation, and the MCMF is used for position matching.

For each tracking target, the number of frames a_k since the last detection result that matches the tracking result is recorded. Once the detection result of a target is correctly associated with the tracking result, this parameter is set to 0. The maximum threshold A_{max} is then set for a_k. If a_k exceeds the set maximum threshold, the tracking process for the target is considered to have ended. When the moving object gradually moves outside the detection range of the Lidar, the tracking of the object ends at this time. When an object in a detection result cannot always be associated with the existing tracker, and the prediction results of the target position of the potential new tracker can be correctly associated with the detection result 5 consecutive times, then the judgment result is the appearance of new objects, avoiding the situation of “false alarms” caused by the jitter of the laser point cloud.

Obstacle status judgment

From the data collected by Beidou navigation equipment, the driving speed V_1 of the tractor is analyzed. Analyze and process the Beidou data, and extract the 10th to 12th places of the Beidou data, that is Ve, Vn, Vu. Use equation (5) to calculate the tractor speed, denoted as V_1:

$$V_1=\sqrt{V_e^{\,2}+V_n^{\,2}+V_u^{\,2}} \tag{5}$$

Obtain the trajectory information and speed information of the obstacle through the target tracking algorithm. The speed information is the sub-velocities in the X_L and Y_L directions in the Lidar coordinate system, and the speed vector V_r and distance S_r. Theoretically, when the obstacle relative to the tractor's speed V_r and the tractor's traveling speed V_1 are numerically equal, the obstacle is considered to be stationary; the rest are considered to be moving. However, in actual situations, due to the measurement error and calculation error of the sensor itself, it is impossible for V_r and V_1 to be completely equal in value, so given a threshold k, when:

$$|V_r|-|V_1|<k \tag{6}$$

The obstacle is considered to be stationary; the rest are considered to be moving. The value of k is determined according to the test of the actual equipment, so that the accuracy of static and dynamic judgments are both above 90%, and the final value is 1.1m/s.

Security warning level division algorithm

This security pre-warning level classification algorithm has different classification models for static obstacles and dynamic obstacles. It is divided into three levels: From level one to level three, the degree of danger gradually decreases.

Static obstacle

Taking the tractor as the research object, and establishing the kinematics model of the tractor, as shown in Figure 5. In the process of tractor driving, the influence of factors such as slip, side slip and ground smoothness are not considered. The model is represented by formula (7) ~ formula (10).

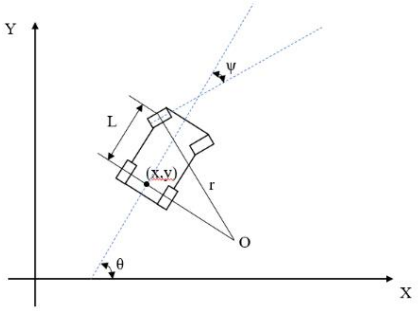

Fig. 5 - Tractor kinematics model

$$\dot{x} = v\cos\theta \tag{7}$$

$$\dot{y} = v\sin\theta \tag{8}$$

$$\dot{\theta}=\omega=\frac{v}{L}\tan\psi \tag{9}$$

$$r = L/\sin\psi \tag{10}$$

where: x and y – the global coordinates of the tractor rear axle center;

θ – The heading angle of the tractor in the global coordinate system (°);

ω – The angular speed of the tractor (rad/s);

v – The driving velocity of the tractor, $v \in (0, v_{max}]$ (m/s);

ψ–The steering angle of the tractor's front wheels (°);

L –The distance between the front and rear wheels of the tractor (m);

r –The turning radius of the tractor (m).

For static obstacles, when the tractor moves forward, the Lidar detects the obstacle, as shown in Figure 6. At this time, the tractor's motion state is estimated according to its kinematics model. $Q(x_k, y_k)$ is the tractor coordinates determined by GNSS at k, and the point $Q'(x_{k+1}, y_{k+1})$ represents the position of the tractor after time ΔT, which is predicted by equation (11).

$$\begin{bmatrix} x_{k+1} \\ y_{k+1} \end{bmatrix} = \begin{bmatrix} x_k \\ y_k \end{bmatrix} + v_k \Delta T \begin{bmatrix} \cos\psi_k \\ \sin\psi_k \end{bmatrix} \tag{11}$$

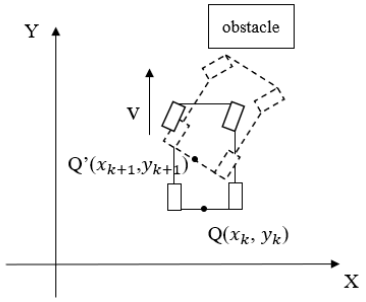

Fig. 6 - Model prediction

When the tractor turns at the maximum turning angle without hitting the obstacle, it is the critical value of turning at this time, that is, the boundary point B of the obstacle is on the trajectory circle where the tractor turns at the maximum turning angle. As shown in Figure 7.

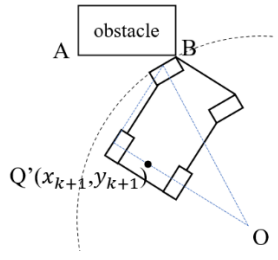

Fig. 7 - Critical condition

From the geometric relationship, the coordinates (a, b) of point O can be obtained, and the circular curve with point O as the center and r as the radius is

$$(x-a)^2+(y-a)^2=r^2 \tag{12}$$

When predicting the trajectory of the tractor, the coordinates of point B(x_B, y_B) are substituted into equation (12) to determine the relationship between point B and point O. As shown in Figure 8, the first-level warning is set to the coordinate of point B within circle 1, the second-level warning is set to the coordinate of point B is within circle 1 and circle 2, and the third-level warning is set to the coordinate of point B is outside circle 2. Among them, circle 2 is concentric with circle 1, and the radius is r+1.

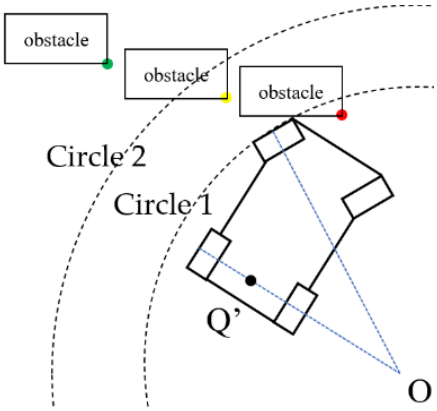

Fig. 8 - Classification of pre-warning levels

Translating it into judging the distance relationship between point B and point O, the following three situations will occur:

$$\sqrt{(x_B-a)^2+(y_B-b)^2}<r \tag{13}$$

$$r<\sqrt{(x_B-a)^2+(y_B-b)^2}<r+1 \tag{14}$$

$$\sqrt{(x_B-a)^2+(y_B-b)^2}<r+1 \tag{15}$$

Then when the coordinate of point B conforms to formula (13), the tractor cannot turn to avoid the obstacle, it is a first-level warning; when the coordinate of point B conforms to formula (14), the tractor can just avoid the obstacle at the maximum turning angle, and it is judged as Second-level early warning; when the coordinate of point B conforms to formula (15), the tractor can avoid the obstacle, and it is judged as a third-level early warning.

Dynamic obstacle

The set safety distance (*Liu et al., 2016*) is the distance required for the tractor to brake to stop. This article sets two levels of safety distance. The first-level safety distance s is the braking distance required for the tractor to decelerate with maximum acceleration. It contains four parts: s_1, s_2, s_3 and s_4. It can be seen from the acceleration change curve in the braking process shown in Figure 9, where s_1 represents the distance traveled by the tractor within t_1 from the time the system sends a signal to the start of the brake. s_2 represents the distance traveled by the tractor within t_2 from the start of the brake action to the time the brake is applied. Therefore, the tractor maintains the initial speed v_1 during the two periods of t_1 and t_2. s_3 represents the distance traveled by the tractor t_3 during the time the brake is applied until the deceleration stabilizes. During t_3, the tractor starts to decelerate, the braking force starts to increase to the maximum, and the deceleration increases. s_4 is the distance traveled by the tractor during the period t_4 when the deceleration is stabilized until the tractor comes to a complete stop. The deceleration reaches its maximum within t_4, and the value remains unchanged to keep the vehicle moving at a constant deceleration. This stage continues until the speed is zero, and the vehicle stops.

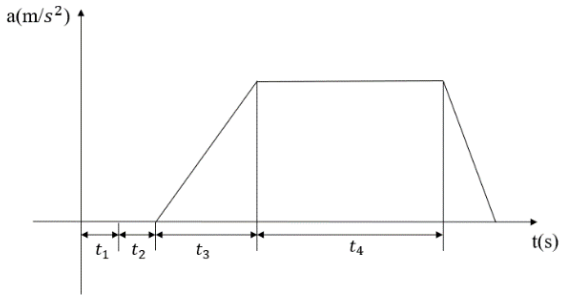

Fig. 9 - Acceleration over time diagram

(1) The above analysis indicates that the tractor moves at a constant speed during t_1 and t_2, thus:

$$s_1 = v_1 t_1 \tag{16}$$

$$s_2 = v_1 t_2 \tag{17}$$

(2) During t_3, the tractor starts to decelerate and the deceleration is increasing. Therefore, the following equation can be used:

$$\frac{dv}{dt} = kt \tag{18}$$

$k = -\frac{a_{\max}}{t_2}$, so $\int dv = \int ktdt$

Since the initial speed of the vehicle at this stage is v_1, so:

$$v_1' = v_1 + \frac{1}{2} k t_3^2 \tag{19}$$

thereby $\frac{ds}{dt} = v_1 + \frac{1}{2} kt^2$, so:

$$\int ds = \int (v_1 + \frac{1}{2} kt^2) dt \tag{20}$$

Initial moment $S = 0$, so:

$$s_3 = v_1 t_3 + \frac{1}{6} k t_3^3 \tag{21}$$

k can then be substituted into the above formula to obtain:

$$s_3 = v_1 t_3 + \frac{1}{6} a_{\max} t_3^2 \tag{22}$$

(3) During t_4, the tractor uses $a_{\max}$ as the deceleration speed to make uniform deceleration motion. At this time, the initial speed is v_1' and the final speed is 0, so:

$$s_4 = \frac{v_1^2}{2a_{\max}} - \frac{v_1 t_3}{2} + \frac{a_{\max} t_3^2}{8} \tag{23}$$

In summary, the expression of s is:

$$s = s_1 + s_2 + s_3 + s_4 \tag{24}$$

$$s = v_1(t_1 + t_2) + \frac{1}{2} v_1 t_3 - \frac{1}{24} a_{\max} t_3^2 + \frac{v_1^2}{2a_{\max}} \tag{25}$$

The second-level safety distance s' is the braking distance required for the tractor to brake at 1/2 of the maximum deceleration. s' also contains four parts: s_1, s_2, s_3 and s_4. The meaning of each section of displacement is the same as the first-level safety distance.

Thus,

$$s' = s_1 + s_2 + s_3 + s_4 \tag{26}$$

$$s' = v_1(t_1 + t_2) + \frac{1}{2}v_1 t_3 - \frac{1}{48}a_{\max}t_3^2 + \frac{v_1^2}{a_{\max}} \tag{27}$$

In the system, t_1 and t_2 are 1.3 s, t_3 is 0.2 s, and a_{max} is 6 m/s^2 according to the actual equipment used.

For dynamic obstacles, the speed V_r of the obstacle relative to the agricultural vehicle is a vector. The forward direction of the agricultural vehicle (i.e. the x direction of the coordinate system) is in the positive direction and vice versa. When the speed is in the positive direction, the obstacle is far away from the agricultural vehicle; thus, no pre-warning is considered. When the speed is in the negative direction, the obstacle is approaching the agricultural vehicle. At this time, the safety warning level is judged.

The collision time is calculated according to the movement state of the agricultural vehicle and the obstacle at the time $t = S_r / V_r$. The distance the tractor travels during this time is $S_t = v_1 t$. S_t is then compared with the two-level safety distance to judge the level. To ensure the unified evaluation of the degree of danger, a pre-warning evaluation index δ is proposed to rank the degree of danger.

Suppose $i = S_t / S$, $j = S_t / S'$

$$\delta = ij \tag{28}$$

δ appears in three situations:

$$\begin{cases} 0 < \delta < 1 \\ j < \delta < i \\ \delta > i \end{cases} \tag{29}$$

When $0<\delta<1$, it is judged as a first-level warning; when $j<\delta<i$, it is judged as a second-level warning; when $\delta>i$, it is judged as a third-level warning.

Real vehicle test

Place static obstacles directly in front of the tractor's forward direction, and through manual tests, determine the position where the tractor cannot go around at the maximum turning angle, the position where the tractor can go around at the maximum turning angle and the distance does not exceed 1m, and the tractor can go around at the maximum turning angle. The positions that pass and the distances differ by more than 1m correspond to the three lines shown in Figure 10. The tractor is driving forward at a speed of 9km/h (±0.8km/h), and the time when the LED warning light is correctly illuminated within each distance is recorded. The experiment was repeated three times for data analysis.

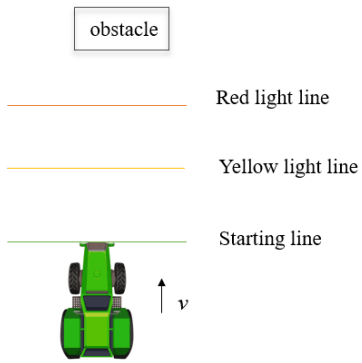

Fig. 10 - Static obstacle test plan

The same site was used to conduct dynamic obstacle tests, and human subjects were used as dynamic obstacles. Tests were conducted both away from and close to the tractor. The tests away from the tractor were conducted as follows: a person walks from the front of the tractor (Figure 11(a)) and the side (Figure 11(b)), including the left and right sides, at a brisk walking speed (1.2–1.4 m•s^{-1}) while staying away from the tractor. The test was run three times in each direction to determine whether the warning light was always green.

The other test was conducted as follows: a person approaches the tractor at a distance from the front walking at a normal speed (1 m/s (±0.3 m•s^{-1})), fast walking speed (2 m/s (±0.3 m•s^{-1})), and jogging speed (3 m/s (±0.3 m•s^{-1})) (Figure 11(c). Tests for each type of speed were repeated three times, and the distance and speed between the person and the tractor when the warning light changes from green to yellow and to red were recorded for data analysis.

(a)Front (b)Side (c) approach

Fig. 11 - Dynamic obstacle test photo

RESULTS AND DISCUSSION

It can be seen from the test results that the early warning accuracy rate of this safety early warning system for static obstacles is over 85.5%, and the early warning effect is good. The green light area has the best effect due to the long distance and long distance, and the error of the Lidar ranging has less influence on it. The yellow light area has the shortest distance. A slight bump of the tractor during driving will cause data instability, which will lead to a decrease in accuracy. Although the distance of the red light area is also short, it is already very close to the obstacle, and the Lidar data error is small, so the accuracy rate has increased.

The test results of static obstacles are shown in the table below.

Table 1

Results of the first test

Times / Result	Correct lighting time / s	Error lighting time / s	Accuracy	Average
Green light area	6.9	0.90	88.5%	85.4%
Yellow light area	1.5	0.30	83.3%	
Red light area	3.8	0.70	84.4%	

Table 2

Results of the second test

Times / Result	Correct lighting time/s	Error lighting time/s	Accuracy	Average
Green light area	6.8	0.8	89.5%	85.7%
Yellow light area	1.8	0.3	85.7%	
Red light area	3.2	0.7	82.1%	

Table 3

Results of the third test

Times / Result	Correct lighting time / s	Error lighting time / s	Accuracy	Average
Green light area	6.5	0.8	89.0%	85.4%
Yellow light area	1.9	0.4	82.6%	
Red light area	3.3	0.6	84.6%	

When dynamic obstacles are far away from the tractor, the warning light is green more than 96.6% of the time, which is consistent with expectation. That is, when the obstacle is far away from the tractor, it is considered safe, and no warning is required.

In 3.4% of the cases, the lights were not turned on correctly because of the effect of the bumpy terrain on the sudden change in tractor speed and the occasional deviation in the speed of BDS.

The test results of people far away from the tractor are shown in Table 4-6:

Table 4

Ahead far away the test results

Times / Result	Correct lighting time / s	Error lighting time / s	Accuracy	Average
The first test	7.9	0	100.0%	98.3%
The second test	8.3	0.2	97.6%	
The third test	7.6	0.2	97.4%	

Table 5

Far away from the left side the test results

Times / Result	Correct lighting time / s	Error lighting time / s	Accuracy	Average
The first test	7.3	0	100.0%	97.9%
The second test	7.5	0.2	97.3%	
The third test	8.1	0.3	96.4%	

Table 6

Far away from the right side the test results

Times / Result	Correct lighting time / s	Error lighting time / s	Accuracy	Average
The first test	7.7	0.1	98.7%	99.6%
The second test	8.4	0	100.0%	
The third test	7.5	0	100.0%	

During the test, the tractor drives forward at the tillage speed of 9 km/h; the first-level safety distance S is 4.3 m, and the second-level safety distance S' is 4.8 m. Based on the results in the above table, 94.4% of the pre-warning distances are consistent with expectations. In the second test of the human subjects walking at normal speeds, S_t when the green light turns to yellow is slightly larger than S', which is caused by the bumps of the tractor during the driving process. In addition, in the test with artificial jogging, the warning light did not appear to be yellow for the first and third repetitions of the test but instead directly changed from green to red. The analysis indicated that the movement of the dynamic obstacles is faster at this time; furthermore, the range of changes in various parameters is greater, the yellow light range is shorter, and there is no yellow light warning. When the dynamic obstacle moves faster, the warning light sends out a red warning signal when the tractor is still far away from the obstacle to provide more time for braking or making a turn. Thus, this system can send out a red warning signal faster based on the speed of the obstacle when the dynamic obstacle is moving rapidly, thus enhancing the safety of operation. To sum up, the pre-warning accuracy of dynamic obstacles is 95.5% for the results of faraway experiment and near experiment. The results of people approaching the tractor are shown in Table 7:

Table 7

Jogging speed test results

	Normal walking speed		Brisk walking speed		Jogging speed	
	Red	Yellow	Red	Yellow	Red	Yellow
The first test	4.16	4.63	3.71	4.46	3.02	-
The second test	3.98	4.82	3.65	4.39	3.14	4.35
The third test	4.03	4.69	3.85	4.55	2.98	-

CONCLUSIONS

This research presents a system suitable for monitoring the surrounding environment of agricultural vehicles that can provide a safety warning and proposes a method to detect obstacles and judge the state of obstacles through Lidar scanning. Different safety pre-warning models are proposed for static and dynamic obstacles. The accuracy of the pre-warning is 90.5% (average value of static obstacle experiment and dynamic obstacle experiment results), and faster obstacles correspond to higher danger and more rapid triggering of alarms.

Compared with previous studies, the parameters of this system can be set according to the actual agricultural vehicles used, which increases its applicability. In addition, this system features a two-level safety distance that can match the degree of danger of different obstacles in more detail. Finally, the motion parameters of obstacles are comprehensively considered rather than simply using distance as the criterion, which improves the accuracy of pre-warning.

However, this study only conducted experimental verification using one type of tractor. Thus, future studies are needed to verify the model using different types of agricultural vehicle tests. Furthermore, the entire safety pre-warning model needs to be modified to accommodate the parameters of different types of agricultural vehicles.

ACKNOWLEDGEMENT

The authors thank the editing team of EditorBar for improving the English language fluency of our paper. The work in this paper was supported by the National Key Research and Development Program (No. 2017YFD0700402), the China Postdoctoral Science Foundation (No. 2019M653764) and the Chinese Universities Scientific Fund (No. 2452018051).

REFERENCES

[1] Asvadi A., Premebi Da C., Peixoto P., et al. (2016). 3D Lidar-based static and moving obstacle detection in driving environments. *Robotics & Autonomous Systems*, pp. 299-311;

[2] Buczkowska S., Coulombel N., et al. (2019). A comparison of Euclidean Distance, Travel Times, and Network Distances in Location Choice Mixture Models. *Networks and Spatial Economics*, vol. 19, no. 4, pp. 1215-1248;

[3] Campos Y., Sossa H. and Pajares G., (2016). Spatio-temporal analysis for obstacle detection in agricultural videos. *Applied Soft Computing Journal*, vol. 45, pp. 86-97;

[4] Cao M.C. and Wang J.M., (2016). Obstacle Detection for Autonomous Driving Vehicles with Multi-Lidar Sensor Fusion. *Journal Of Dynamic Systems Measurement and Control-Transactions of the ASME*, vol. 142, no. 2;

[5] Chen X.X., Wu H., Wu Y.W., et al. (2017), Large-Scale Resource Scheduling Based on Minimum Cost Maximum Flow (基于最小成本最大流量的大规模资源调度), *Journal of Software*, vol. 28, no. 3, pp. 598-610;

[6] Jeong E., Oh C. and Lee G. (2015). Emission evaluation of inter-vehicle safety warning information systems. *Transportation Research Part D: Transport and Environment*, vol. 41, no. 12, pp. 106-117;

[7] Corno M., Furioli S., Cesana P., et al., (2021). Adaptive Ultrasound-Based Tractor Localization for Semi-Autonomous Vineyard Operations. *Agronomy*, vol. 11, no. 2, pp. 287;

[8] García-Martínez H., Flores-Magdaleno H., Ascencio-Hernández R. et al. (2020). Corn Grain Yield Estimation from Vegetation Indices, Canopy Cover, Plant Density, and a Neural Network Using Multispectral and RGB Images Acquired with Unmanned Aerial Vehicles, *Agriculture*, vol. 10, no. 7, pp. 277;

[9] Guo, C.Y., Zhao X., Zhang S., et al. (2019). Design of a cross-boundary warning system for soil preparation based on bds, *INMATEH-Agricultural Engineering*, vol. 59, no. 3, pp. 59-68;

[10] Kapilan K., Bandara S. and Dammalage T., (2020). Vehicle Accident Detection and Warning System for Sri Lanka Using GNSS Technology. in 1st International Conference on Image Processing and Robotics, ICIPRoB 2020, March 6, 2020 - March 8, 2020. *Negombo, Sri Lanka: Institute of Electrical and Electronics Engineers Inc*;

[11] Liang Y.Y., Liu X.H., He Z.Y. et al. (2019). Multiple objects tracking by reliable tracklets. *Signal Image and Video Processing*, vol. 13, no. 4, pp. 823-831;

[12] Liu G.R., Zhou M.Z., Wang L.L., et al. (2016). Control model for minimum safe inter-vehicle distance and collision avoidance algorithm in urban traffic condition. *Automotive Engineering,* vol. 38, no. 10, pp. 1200-5+1176.
[13] Liu M.C., (2018). Research on inspection and obstacle avoidance methods of agro-machinery obstructions (农机障碍物检测与避障方法研究), *Northwest A&F Univ*;
[14] Liu Q., Qiu X.X., Xie L.M., et al. (2017). Anti-collision warning time algorithm based on driving speed of vehicle(基于车速的车辆碰撞预警时间算法), *Transactions of the Chinese Society of Agricultural Engineering*, vol. 33, no. 12, pp. 99-106;
[15] Loukatos D., Petrongonas E., Manes K., et al. (2021). A Synergy of Innovative Technologies towards Implementing an Autonomous DIY Electric Vehicle for Harvester-Assisting Purposes, *Machines*, vol. 9, no. 4, pp. 82;
[16] Sun Q., Huang L.S., Guo W.J., et al. (2014), Content-aware association control in wireless networks. *Journal of Computational Information Systems*, vol. 10, no. 7, pp. 2865-2872;
[17] Tak S., Yoon J., Woo S., et al. (2020). Sectional Information-Based Collision Warning System Using Roadside Unit Aggregated Connected-Vehicle Information for a Cooperative Intelligent Transport System, *Journal of Advanced Transportation*, pp. 1-12;
[18] Wojke N., Bewley A., Paulus D., et al. (2017). Simple online and realtime tracking with a deep association metric. *24th IEEE International Conference on Image Processing*, ICIP 2017, September 17, 2017 - September 20, 2017. Beijing, China: IEEE Computer Society;
[19] Yan W.Y., Salem M., Ahmed S., et al. (2016). Automatic extrajction of highway light poles and towers from mobile Lidar data. *Optics And Laser Technology*, vol. 77, pp. 162-168;
[20] Zhang Y.H., Geng G.H.,Wei X.R.,et al. (2017). Feature extraction of point clouds using the DBSCAN clustering(基于DBSCAN聚类的点云特征提取), *Journal of Xidian University*, vol. 44, no. 2, pp. 114-120;
[21] Zhao X. (2019). Study on the cross-boundary warning system of soil preparation based on BDS (基于BDS的整地跨界预警系统研究), *Northwest A&F Univ*;
[22] Zhu, T.J., Zong C.F., Wu B.S., et al. (2011). Rollover warning system of heavy-duty vehicle based on improved TTR algorithm (基于改进TTR算法的重型车辆侧翻预警系统), *Journal of Mechanical Engineering*, vol. 47, no. 10, pp. 88-94.